A&A 636, A72 (2020)
https://doi.org/10.1051/0004-6361/201936981

Astronomy & Astrophysics

Kernel-phase analysis: Aperture modeling prescriptions that minimize calibration errors

Frantz Martinache[1], Alban Ceau[1], Romain Laugier[1], Jens Kammerer[2,3], Mamadou N'Diaye[1], David Mary[1], Nick Cvetojevic[1], and Coline Lopez[1]

[1] Université Côte d'Azur, Observatoire de la Côte d'Azur, CNRS, Laboratoire Lagrange, Nice, France
e-mail: frantz.martinache@oca.eu
[2] European Southern Observatory, Karl-Schwarzschild-Str 2, 85748 Garching, Germany
[3] Research School of Astronomy & Astrophysics, Australian National University, Canberra, ACT 2611, Australia

Received 24 October 2019 / Accepted 4 March 2020

ABSTRACT

Context. Kernel phase is a data analysis method based on a generalization of the notion of closure phase, which was invented in the context of interferometry, but it applies to well corrected diffraction dominated images produced by an arbitrary aperture. The linear model upon which it relies theoretically leads to the formation of observable quantities robust against residual aberrations.
Aims. In practice, the detection limits that have been reported thus far seem to be dominated by systematic errors induced by calibration biases that were not sufficiently filtered out by the kernel projection operator. This paper focuses on the impact the initial modeling of the aperture has on these errors and introduces a strategy to mitigate them, using a more accurate aperture transmission model.
Methods. The paper first uses idealized monochromatic simulations of a nontrivial aperture to illustrate the impact modeling choices have on calibration errors. It then applies the outlined prescription to two distinct data sets of images whose analysis has previously been published.
Results. The use of a transmission model to describe the aperture results is a significant improvement over the previous type of analysis. The thus reprocessed data sets generally lead to more accurate results, which are less affected by systematic errors.
Conclusions. As kernel-phase observing programs are becoming more ambitious, accuracy in the aperture description is becoming paramount to avoid situations where contrast detection limits are dominated by systematic errors. The prescriptions outlined in this paper will benefit from any attempt at exploiting kernel phase for high-contrast detection.

Key words. instrumentation: high angular resolution – methods: data analysis – stars: low-mass – binaries: visual

1. Introduction

Within the anisoplanetic field of an imaging instrument, and in the absence of saturation, an in-focus image I can formally be described as the result of a convolution product

$$I = O \star \mathrm{PSF} \tag{1}$$

between the spatially incoherent brightness distribution of an object O and the instrumental point spread function (PSF). The careful optical design of telescopes and instruments assisted by adaptive optics (AO) attempts to bring the PSF as close as possible to the theoretical diffraction limit. Yet even for high quality AO correction, subtle temporal instabilities in the PSF make it difficult to solve for important problems, such as the following: the identification of faint sources or structures in the direct neighborhood of a bright object (the high-contrast imaging scenario) or the discrimination of sources that are close enough to one another to be called nonresolved (the super-resolution scenario). Weak signals of astrophysical interest compete with time-varying residual diffraction features that render the deconvolution difficult.

The overall purpose of interferometric processing of diffraction-dominated images is to provide an alternative to the otherwise ill-posed image deconvolution problem. The technique takes advantage of the properties of the Fourier transform, which turns the convolution into a multiplication. One must, however, abandon the language describing images and instead manipulate the modulus, which is also referred to as the visibility, and the phase of their Fourier transform counterpart. This Fourier transform can be sampled over a finite area of the Fourier plane traditionally described using the (u, v) coordinates, whose extent depends on the geometry of the instrument pupil.

Nonredundant masking (NRM) interferometry uses a custom aperture mask featuring a finite number of holes that considerably simplifies the interpretation of images. Accurate knowledge of the mask's subaperture locations unambiguously associates particular complex visibility measurements in the image's Fourier transform to specific pairs of subapertures forming a baseline. The Fourier phase Φ at the coordinate (u, v) is the argument of a single phasor:

$$\phi(u,v) = \mathrm{Arg}\left(v_0(u,v)e^{i(\phi_0(u,v)+\Delta\varphi(u,v))}\right) \tag{2}$$

$$= \Phi_0(u,v) + \Delta\varphi(u,v), \tag{3}$$

where $v_0(u, v)$ and $\phi_0(u, v)$ represent the intrinsic target visibility modulus and phase for this baseline, respectively, and $\Delta\varphi(u, v)$ is the instrumental phase difference (i.e., the piston) experienced by the baseline at the time of acquisition. The same geometrical knowledge also makes it possible to combine complex visibility measurements by baselines forming closing-triangles, which lead to the formation of closure phases, which are observable quantities engineered to be insensitive to differential piston errors affecting the different baselines.

The closure phase was first introduced in the context of radio interferometry by Jennison (1958) and eventually exploited in the optical starting with Baldwin et al. (1986). This useful observable enables NRM interferometry to detect companions at smaller angular separations than a coronagraph can probe.

Kernel-phase analysis attempts to take advantage of the same property without requiring the introduction of a mask. The description of the full aperture requires a more sophisticated model that reflects the intrinsically redundant nature of the aperture. Any continuous aperture can be modeled as a periodic grid of elementary subapertures, resulting in a virtual interferometric array where every possible pair of subapertures forms a baseline. Whereas the NRM ensures that each baseline is only sampled once, the regular grid results in a highly redundant scenario. For a baseline of coordinate (u, v) and redundancy R, the Fourier phase is that of the sum of R phasors that all measure the same $\phi_0(u, v)$ but experience different realizations of instrumental phase $(\Delta\varphi_k)_{k=1}^{R}$:

$$\phi(u, v) = \mathrm{Arg}\left(\sum_{k=1}^{R} v_0(u, v) e^{i(\phi_0(u,v)+\Delta\varphi_k)}\right). \quad (4)$$

In the low-aberration regime provided by modern AO systems, the impact the residual pupil aberration φ has on the Fourier phase can be linearized and Eq. (4) can be rewritten as:

$$\phi(u, v) = \phi_0(u, v) + \frac{1}{R}\sum_{k=1}^{R} \Delta\varphi_k. \quad (5)$$

The list of what pairs of subapertures contribute to the complex visibility of a redundant baseline is kept in the baseline mapping matrix $\mathbf{A}$. It contains as many columns as there are subapertures (n_A) and as many rows as there are distinct baselines (n_B). Elements in a row of $\mathbf{A}$ are either 0, 1, or -1 (see Fig. 1 of Martinache 2010). The phase that is sampled at all relevant coordinates of the Fourier-plane and gathered into a vector Φ, can thus be written compactly as:

$$\Phi = \Phi_0 + \mathbf{R}^{-1} \cdot \mathbf{A} \cdot \varphi, \quad (6)$$

where $\mathbf{R}$ is the diagonal (redundancy) matrix that retains the tally of how many subaperture pairs contribute to the Fourier phase for that baseline, φ is the aberration experienced by the aperture, and Φ_0 is the Fourier phase associated with the object being observed; it is related to the object function O of Eq. (1) by the Van-Cittert Zernike theorem. The redundancy $\mathbf{R}$ is expected to be directly proportional the modulus transfer function (MTF) of the instrument. The product $\mathbf{R}^{-1} \cdot \mathbf{A}$, referred to as the phase transfer matrix, describes the way pupil phase aberration propagate into the Fourier plane. The baseline mapping and the phase transfer matrices are rectangular and feature n_B rows (the number of baselines) for n_A columns (the number of subapertures in the pupil), with $n_\mathrm{B} > n_\mathrm{A}$.

As shown in Martinache (2010), selected linear combinations of the rows of the phase transfer matrix cancel the effect of the pupil phase φ out. These linear combinations, which are gathered into an operator called $\mathbf{K}$ (the left-hand null space or kernel of the phase transfer matrix), project the Fourier phase onto a subspace that is theoretically untouched by residual aberrations. The resulting observables, called kernel phases, are a generalization of the concept of closure phase, which can be found for an arbitrary pupil, regardless of the level of redundancy.

Practice suggests that the kernel and closure phase do not self-calibrate perfectly. Recently published studies using kernel phase to interpret high-angular resolution, diffraction-dominated observations indeed lead to contrast detection limits, which are mostly constrained by systematic errors (Kammerer et al. 2019; Laugier et al. 2019; Sallum & Skemer 2019) instead of statistical errors (Ceau et al. 2019). The goal of this paper is to provide insights into the limitations of Fourier phase methods, in general, and to introduce the means by which to improve upon these limitations.

This difficulty affects the kernel-phase interpretation of images as well as that of NRM interferograms. Despite the generalized assistance of AO during NRM observations (Tuthill et al. 2006), the need for long integration times and the use of subapertures that are not infinitely small means that interferograms are not simply affected by a simple and stable piston, but by a time-varying higher order amount of aberration (Ireland 2013). Closure phases, which are thus acquired on a point source, therefore rarely reach zero and are biased.

Nevertheless, even when evolving over time, if the spatial and temporal properties of the perturbations experienced by the system remain stable across the observation of multiple objects, the overall resulting bias is also expected to remain stable. It is therefore possible to calibrate the closure phases acquired on a target of interest with those acquired on a point-source. Thus calibrated closure phases have been used as the prime observable for the detection of low to moderate contrast companions (Kraus et al. 2008). There is, however, a limit to the stability of the observing conditions when moving from target to target: Changes in elevation, apparent magnitude for the AO, and telescope flexures result in the evolution of the closure-phase bias. Therefore, in practice, the observations never calibrate perfectly and the evolution of the calibration bias results in what is generally referred to as a systematic error.

For low-to-moderate contrast detections up to a few tens, systematic errors are often a minor contribution that do not significantly affect the interpretation of the data. However, as observing programs become more ambitious, attempting the direct detection of higher contrast companions (Kraus & Ireland 2012) in a part of the parameter space that cannot be probed by coronagraphic techniques yet, systematic errors become more important than statistical errors and one must resort to more advanced calibration strategies using multiple calibrators (Ireland 2013; Kammerer et al. 2019) to better estimate the calibration bias that minimizes the amount of systematic error.

2. Fourier phase calibration errors

Kernel-phase analysis requires approximating the near-continuous aperture of the telescope by a discrete representation: A virtual array of subapertures, which are laid on a regular grid of a predefined pitch s, paves the surface covered by the original aperture. The computation of all the possible pairs of virtual subapertures in the array leads to the creation of a second grid of virtual baselines, the majority of which are highly redundant. An example is shown in Fig. 1 for the aperture of an 8 m telescope, which is discretized with a grid of pitch $s = 42$ cm. Keeping track of what pairs of subapertures contribute to all the baselines leads to the computation of the baseline mapping matrix $\mathbf{A}$ and the redundancy matrix $\mathbf{R}$. The two are used to eventually determine the kernel operator $\mathbf{K}$ that generalizes the notion of closure phase, as introduced by Martinache (2010).

The following simulation illustrates the interest of this line of reasoning. Using a single, simulated, monochromatic ($\lambda = 1.6\,\mu$m), and noise-free image of a 10:1 contrast binary object (located two resolution elements to the left of the primary) that is

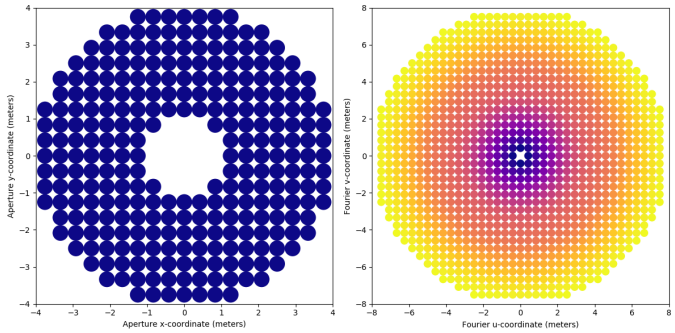

Fig. 1. Binary discrete representation of the SCExAO instrument pupil for kernel-phase analysis. *Left panel*: dicretized instrument pupil built from a square grid of pitch $s = 42$ cm. *Right panel*: Fourier coverage associated with this discretization. The color code used to draw the Fourier coverage reflects the redundancy associated with the virtual interferometric baselines.

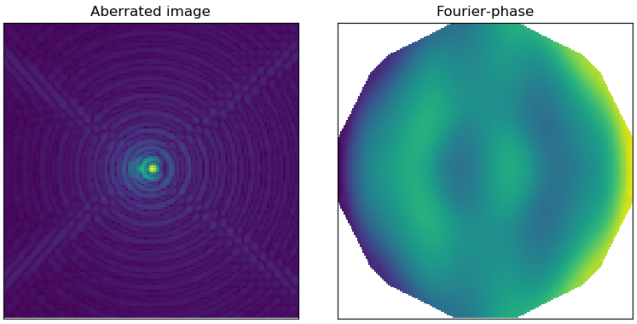

Fig. 2. *Left*: simulated monochromatic ($\lambda = 1.6\,\mu$m) SCExAO image of a 10:1 binary in the presence of 100 nm of coma along the axis of the binary. *Right*: associated Fourier phase ranging from ±1.5 radian (see also Fig. 3).

affected by a fairly large (100 nm rms) amount of coma is shown in the left panel of Fig. 2. The Fourier phase Φ extracted from this image (shown in the right panel of Fig. 2) appears to be completely dominated by the aberration. The plot of the same raw Fourier phase (the blue curve in the top panel of Fig. 3) compared to the predicted Fourier signature of the sole binary Φ_0 confirms this observation. By using the kernel operator $\mathbf{K}$ computed according to the properties of the discrete model[1] represented in Fig. 1, it is possible to project the 546-component noisy Fourier phase vector Φ onto a subspace that results in the formation of a 414-component kernel. The bottom panel shows how, despite the drastic difference between the raw and theoretical Fourier phase, the two resulting kernels match one another: The kernel operator effectively erases the great majority of the aberrations affecting the phase present in the Fourier space, while leaving enough information to describe the target in a meaningful manner, such that:

$$\mathbf{K} \cdot \Phi = \mathbf{K} \cdot \Phi_0. \tag{7}$$

Although the application of $\mathbf{K}$ strongly reduces the impact of the aberration, the match between the kernel curves is not perfect. The small difference between the two example curves is what is generally referred to as the calibration error. This error can be independently measured using the image of a point source

[1] The model was computed using a python package called XARA, which was developed in the context of the KERNEL project, and is available for download http://github.com/fmartinache/xara/

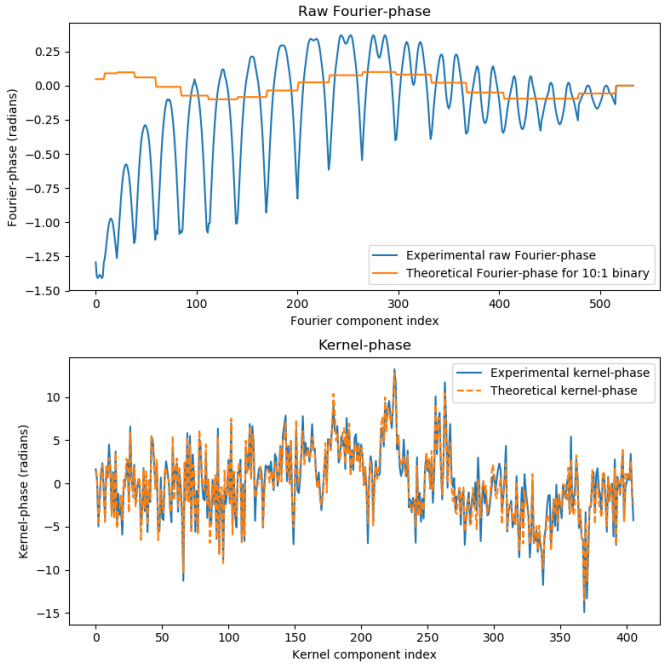

Fig. 3. Demonstration of the impact of the kernel processing. *Top panel*: experimental Fourier phase extracted from a single aberrated image shown in Fig. 2 (the blue curve) bears little ressemblance with the theoretical expected binary signal (in orange). Contrasting with the raw Fourier phase, the *bottom panel* shows how the projection onto the kernel subspace efficiently erases the impact of the aberration and brings the experimental kernel-phase curve ($\mathbf{K} \cdot \Phi$), which is also plotted with a solid blue line, much closer to its theoretical counterpart ($\mathbf{K} \cdot \Phi_0$), which is now plotted with a dashed orange line so as to better distinguish them.

(a calibrator), assuming that the system suffers from the same aberration. In this noise-free scenario, the subtraction of the kernel phase extracted from one such calibration image would result in a perfect match. An instrumental drift between the two exposures would result in a new bias. If the magnitude of this new bias becomes comparable to or larger than the statistical uncertainties; the interpretation of the kernel and closure phase typically requires invoking a tunable amount of systematic error added in quadrature to the uncertainty.

3. Kernel phase discretization prescriptions

Given that no noise was included in this ideal scenario, the fact that some aberration leaks into the kernel and results in the need for calibration suggests that the discrete model used to describe how pupil phase propagates into the Fourier plane is not sufficiently accurate. Thus, we look into ways to improve it.

3.1. Building a discrete representation

The discretization process is as follows: A high-resolution 2D image of the aperture is generated from the details of the pupil specifications (outer and inner diameter, spider thickness, angle, and offset). A square grid of subapertures of pitch s is laid atop the pupil image and the points that fall within the open parts of the aperture are kept in the model. To be counted amongst the virtual subapertures, the area of the transmissive part of the original aperture that overlaps with the region covered by the square virtual subaperture has to be greater than 50%. When building the model, it is critical to ensure that no virtual baseline is greater